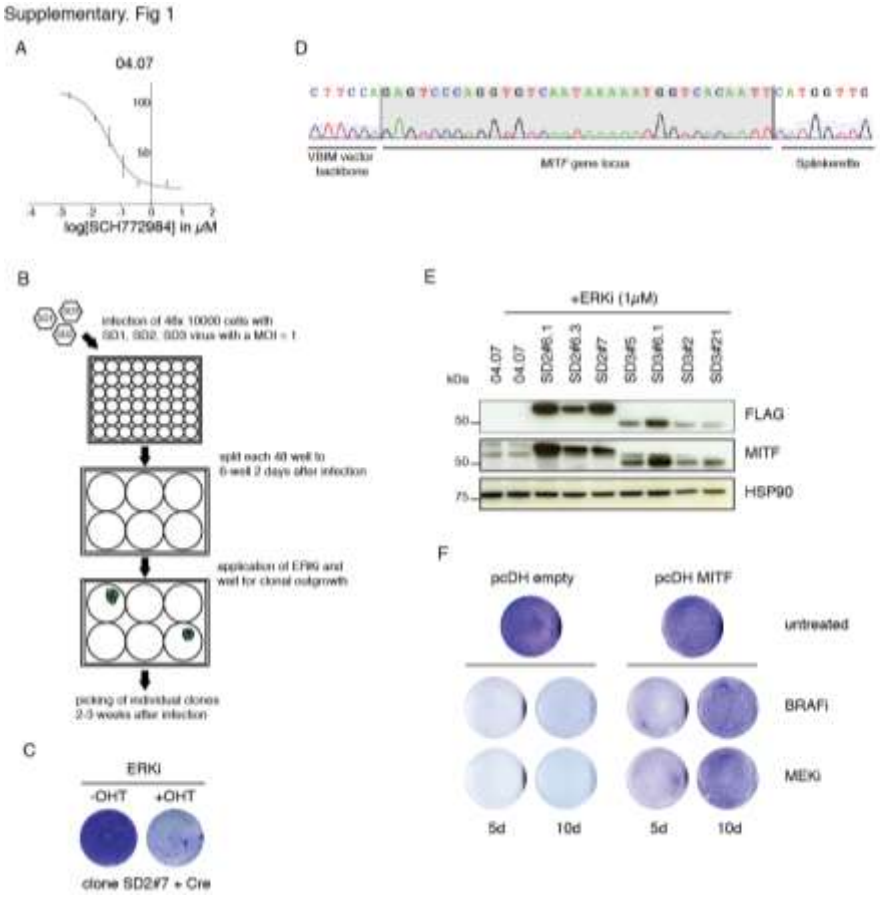

Supplementary Figure 1

A: Sensitivity to ERKi SCH772984 of a low passage BRAF mutant melanoma cell line was measured after three days treatment in a dose response curve. Y-axis represents the percentage of living cells. **B:** Schematic overview of the VBIM screen setup. **C:** Insertion was excised by activation of Cre after addition of 4-OHT, resulting in re-sensitization to SCH772984 as determined by crystal violet staining (representative example is shown). **D:** Sequencing of clone SD3#5 after splinkerette-PCR identified insertion in *MITF* gene locus in intron 2/3. **E:** Immunoblotting of a subset of clones revealed expression of FLAG-tagged proteins, correlating with increased MITF expression. HSP90 served as a loading control. **F:** Lentiviral overexpression of MITF resulted in increased resistance to BRAFi (PLX4720, 5µM) or MEKi (0.5µM) in 04.07 cells as shown by crystal violet staining after five and ten days.

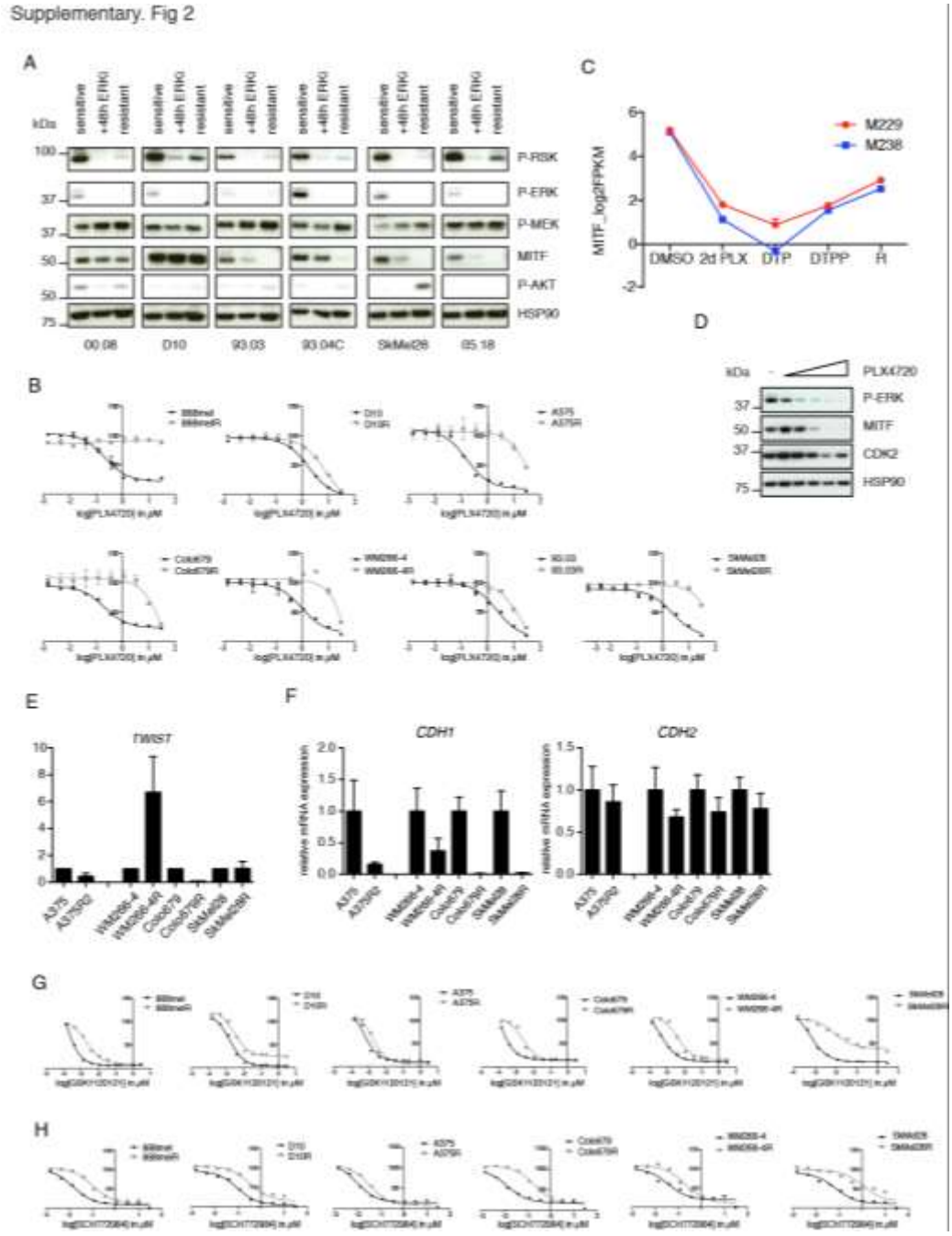

Supplementary Figure 2

A: Immunoblotting of several ERKi (SCH772984)-resistant cell lines and their treatment-naïve counterparts. HSP90 served as a loading control. **B:** Dose response curves of PLX4720-resistant melanoma cell lines and their treatment-naïve counterparts to PLX4720 treatment. Y-axis represents the percentage of living cells. **C:** MITF expression was monitored in M229 and M238 cells starting from initial treatment with PLX4720 to acquisition of resistance. **D:** Colo679 cells were exposed to increasing concentrations of PLX4720 for four days and cell extracts were blotted for the indicated

antibodies. HSP90 served as a loading control. **E:** *TWIST* mRNA was measured in acquired PLX-4720-resistant cells and their treatment-naïve counterparts. Error bars are based on biological replicates and normalized to *RPL13.* **F:** *CDH1* and *CDH2* mRNAs were measured in acquired PLX4720-resistant cells and their treatment-naïve counterparts. Error bars are based on technical replicates and normalized to *RPL13.* **G/H:** Dose response curves of PLX4720-resistant melanoma cell lines and their treatment-naïve counterparts to MEK inhibitor (G) and ERK inhibitor (H) treatment. Y-axis represents the percentage of living cells.

Supplementary. Fig 3

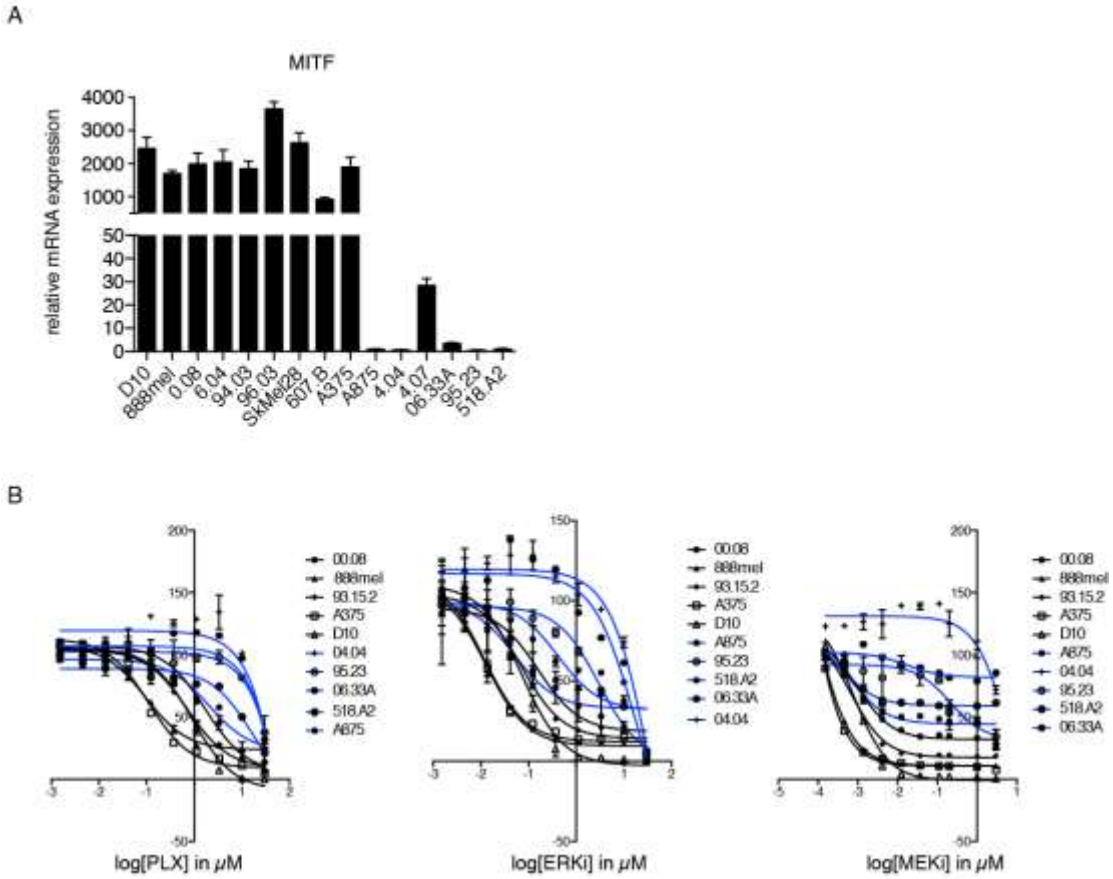

Supplementary Figure 3

A: *MITF* mRNA expression in different BRAF mutant melanoma cells normalized to *ACTINB*. Error bars represent technical replicates. **B:** $MITF^{endo\_hi}$ (black) and $MITF^{endo\text{-}lo}$ (blue) treatment-naïve $BRAF^{V600E}$ melanoma cells were exposed to different concentrations of PLX4720, ERKi or MEKi in a three day-dose response curve.

Supplementary Fig. 4

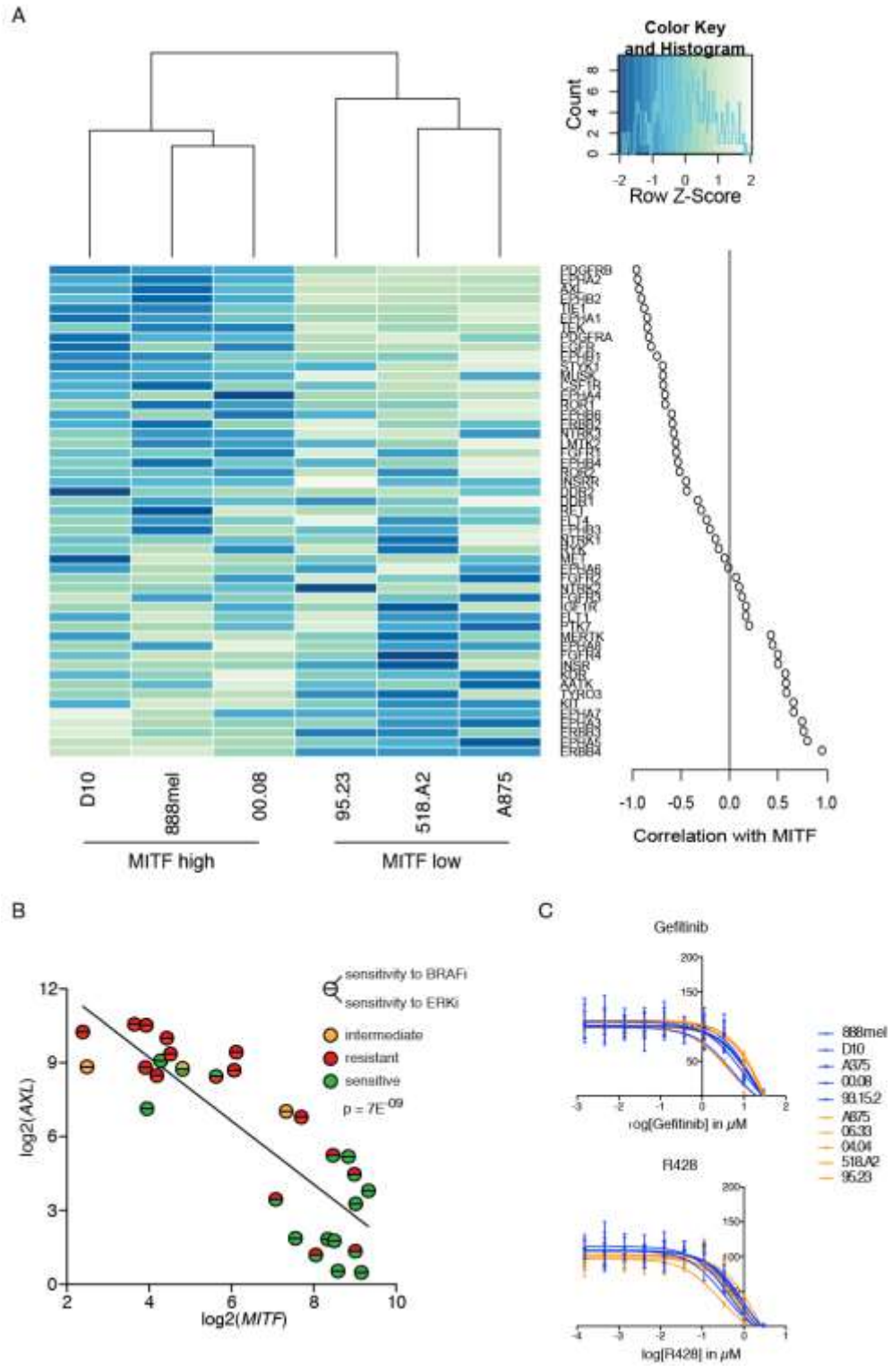

Supplementary Figure 4

A: RNA sequencing was performed on three MITF^{endo_hi} and three MITF^{endo_lo} BRAF^{V600E} mutant melanoma cell lines. The heatmap is based on all RTKs; genes were ordered according to their correlation to MITF. **B:** An independent set of BRAF^{V600E} mutant melanoma cell lines was plotted based on MITF and

AXL expression. Their sensitivities to BRAFi (vemurafenib) and to ERKi SCH772984 are indicated by color codes. The AXL vs. MITF correlation p-value is $7E^{-09}$ and the ERKi sensitivity p-value $3E^{-05}$. **C:** A panel of melanoma cell lines was exposed to either gefitinib or R428 and drug sensitivity was measured in a drug dose response curve after three days. Y-axis represents the percentage of living cells.

Supplemetary. Fig 5

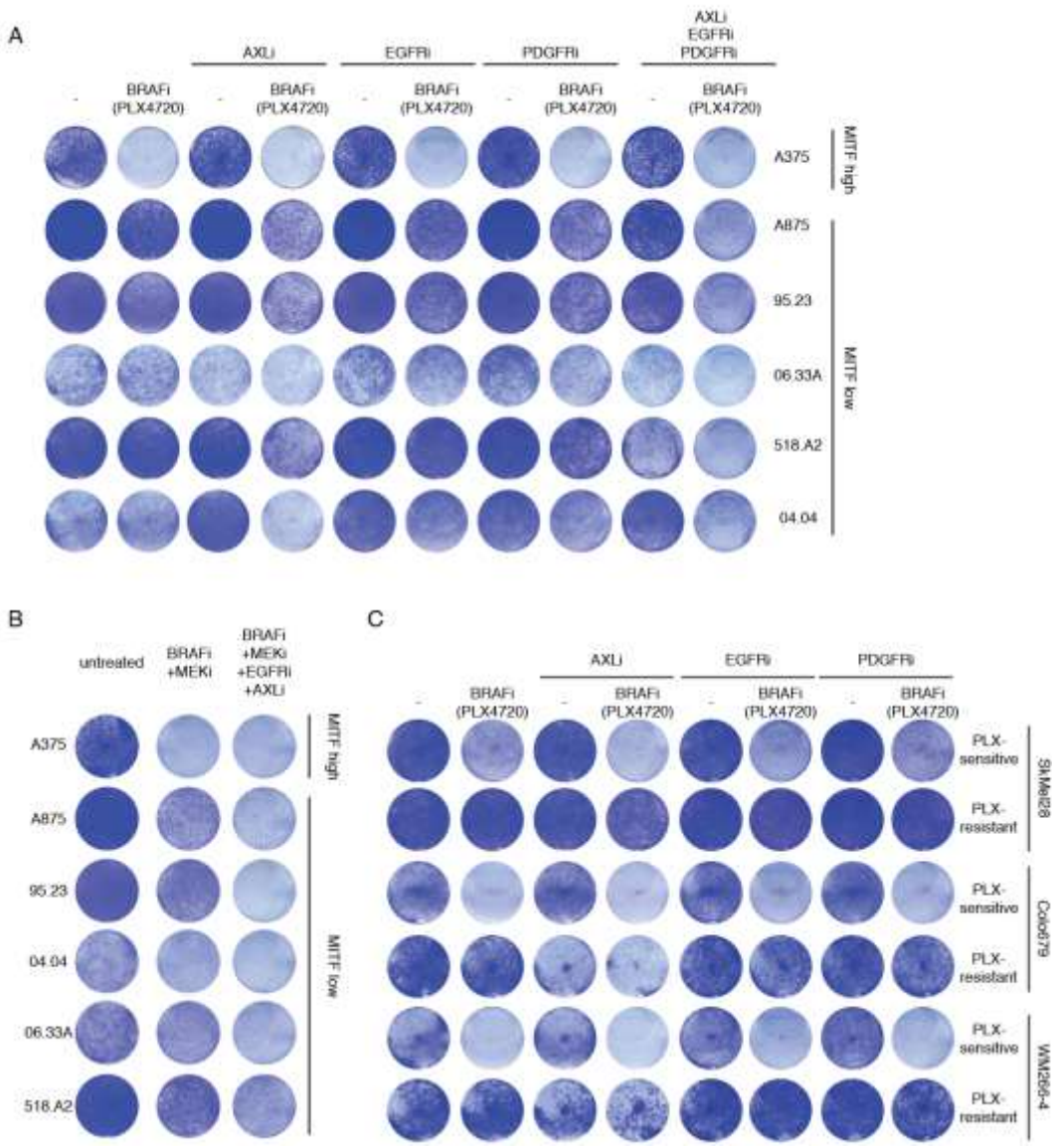

Supplementary Figure 5

A: Five MITF^{endo_lo} and one MITF^{endo_hi} BRAF mutant melanoma cell lines were exposed to a combination of BRAFi PLX4720 with either AXLi R428 (0.3µM), EGFRi Gefitinib (2µM), PDGFRi Imatinib (1µM) or a combination of all for nine days. A375 cells were used as a control for efficient BRAFi treatment. Remaining cells were stained with crystal violet. **B:** MITF^{endo_lo} cells were exposed to a combined inhibition of the MAPK-pathway by BRAFi dabrafenib (2µM) and MEKi trametinib (0.05µM) with combined AXL (R428, 0.3µM) and EGFR (Gefitinib, 2µM) inhibition. After nine days of combined treatment the remaining cells were stained with crystal violet. A375 cells were used as a control for efficient MAPK-pathway inhibition. **C:** Three MITF^{acq_lo} PLX4720-resistant cells lines and their treatment-naïve counterparts were

exposed to AXLi R428 (0.3µM), EGFRi gefitinib (2µM) or PDGFRi imatinib (1µM) for nine days in the presence or absence of PLX4720 (3µM). Remaining cells were stained with crystal violet.

Supplemetary Fig. 6

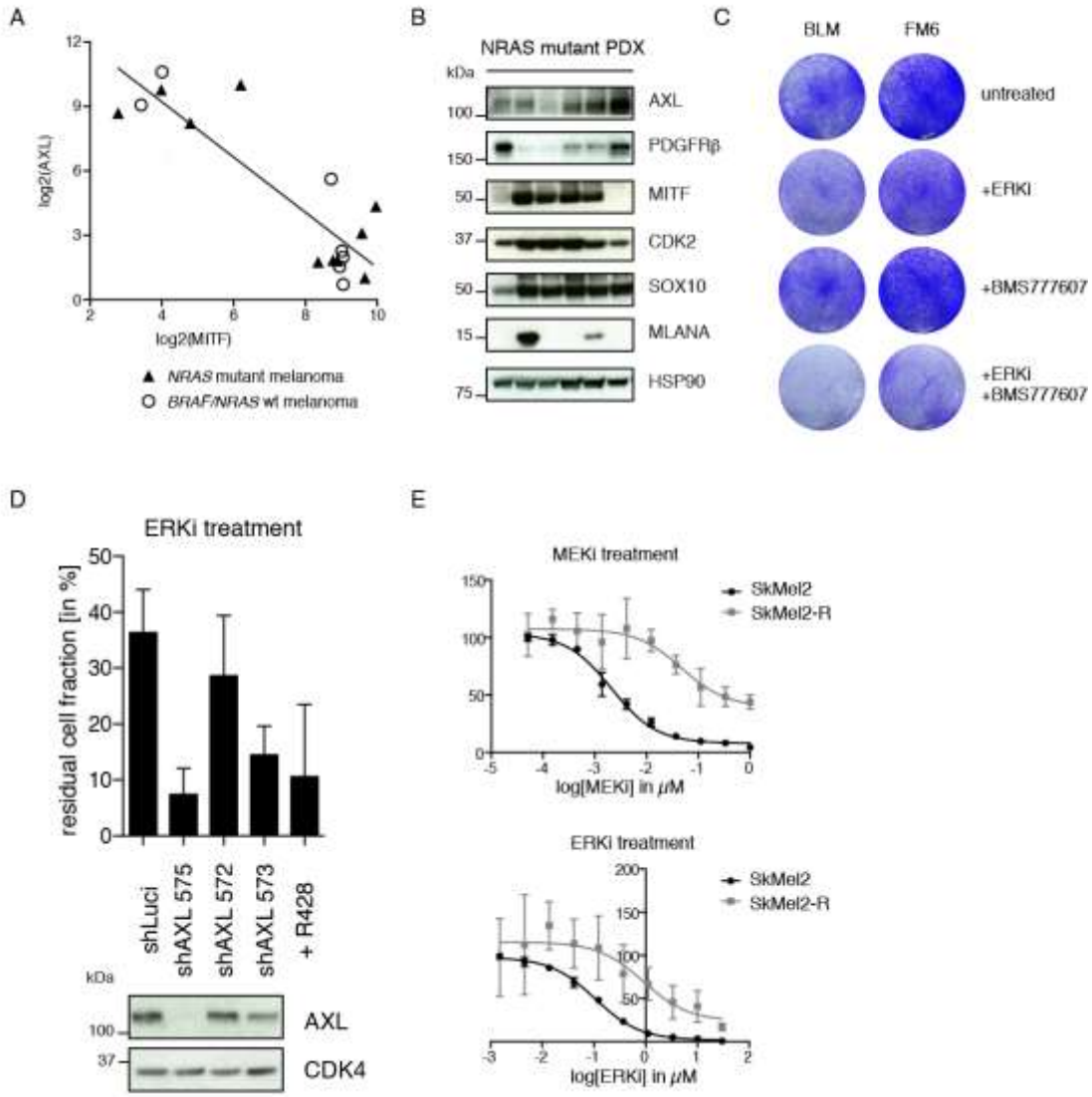

Supplementary Figure 6

A: An independent set of NRAS mutant and BRAF/NRAS wild-type melanoma cell lines was plotted based on *MITF* and *AXL* mRNA expression. **B:** NRAS mutant, treatment-naïve PDX samples were analyzed by immunoblotting for the indicated proteins. HSP90 served as a positive control. **C:** FM6 and BLM cells were plated at low densities and treated with ERKi (1µM), BMS777607 (5µM) or a combination. After six days of treatment remaining cells were stained by crystal violet. **D:** FM6 cells were lentivirally transduced with shRNAs to knock down AXL expression. Efficient knockdown was confirmed by immunoblot (lower panel). AXL knockdown decreased viability of the ERKi-resistant population as measured by dose response curve. Error bars result from three independent experiments. **E:** Dose response curves of SkMel2 and SkMel2R confirmed resistance to MEKi and cross-resistance to ERKi.

Supplementary figure 7: raw images

Figure 1A (left blot, FLAG)

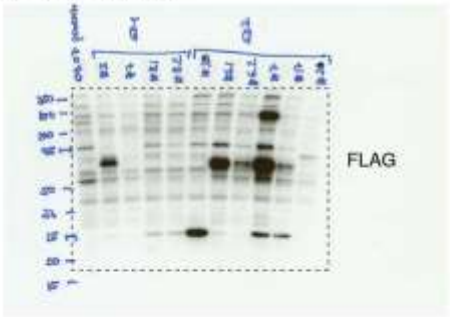

Figure 1A (right blot, FLAG)

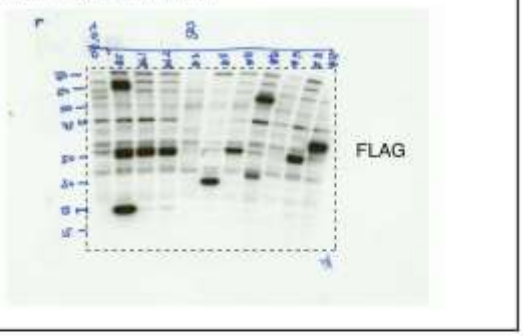

Figure 1D (HSP90, MITF, p-ERK (from top to bottom)

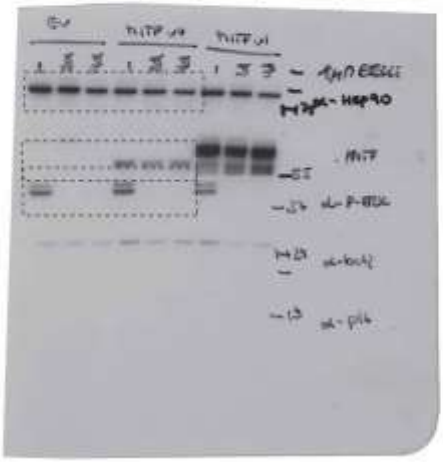

Figure 2B (HSP90, MITF, CDK2, SOX10 (from top to to bottom) in 888mel, SkMel28, A375, 93.03 (left to right))

Figure 2B (P-RSK, P-ERK, MELANA (from top to bottom) in 888mel (P/R), A375 (P/R1/R2), D10 (P/R), SKMel28 (P/R), 93.03 (P/R), Colo679 (P/R), WM266-4 (P/R) (from left to right)

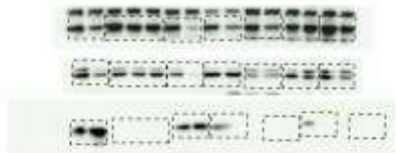

Figure 2B (MITF, SOX10, CDK2, HSP90 (from top to bottom) in Colo679 (P/R), WM266-4 (P/R) (from left to right)

Figure 2B (MITF, SOX10, HSP90, CDK2 (from top to bottom) in D10 (P/R))

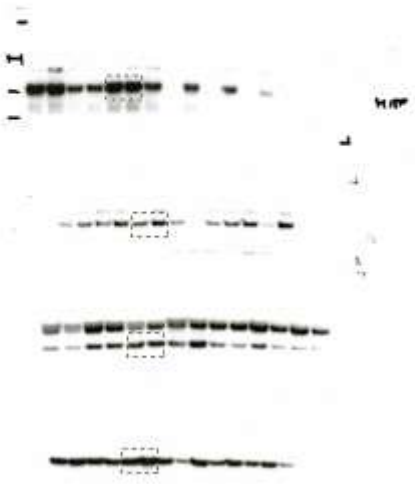

Figure 3B (PARP, P-ERK (from top to bottom) in SkMel28 (top) and PARP, P-ERK (from top to bottom) in 888Mel (bottom))

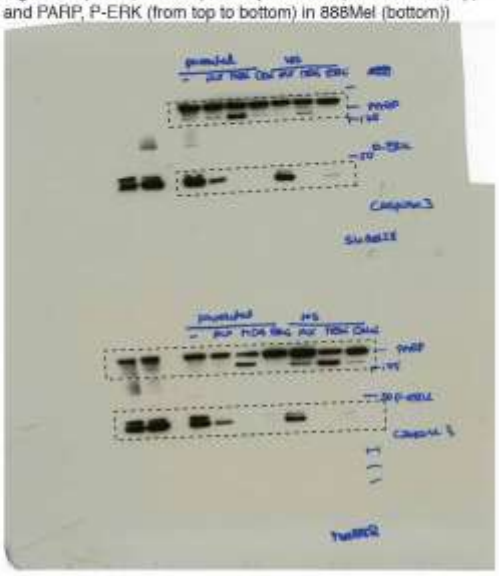

Figure 3B (CDK4 in SkMel28 (top) and CDK4 in 888Mel (bottom))

Figure 3B (MITF in 888Mel (top) and MITF in SkMel28 (bottom))

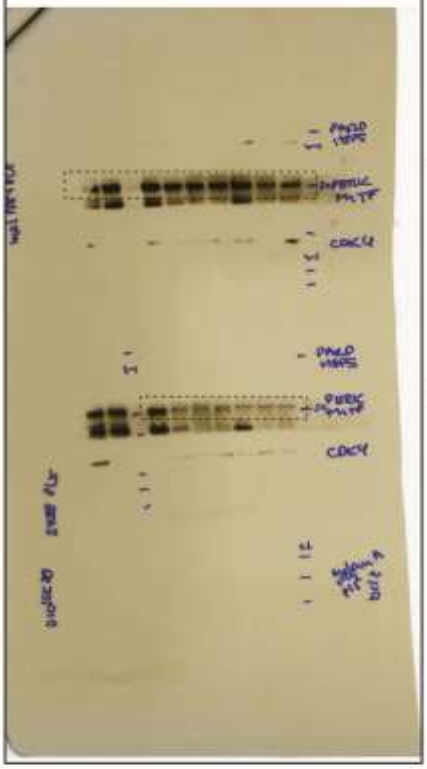

Figure 4C (E-Cadherin in 888Mel (P/R), A375(P/R), D10(P/R), SkMel28(P/R), Colo679(P/R), WM266-4 (P/R) (left to right))

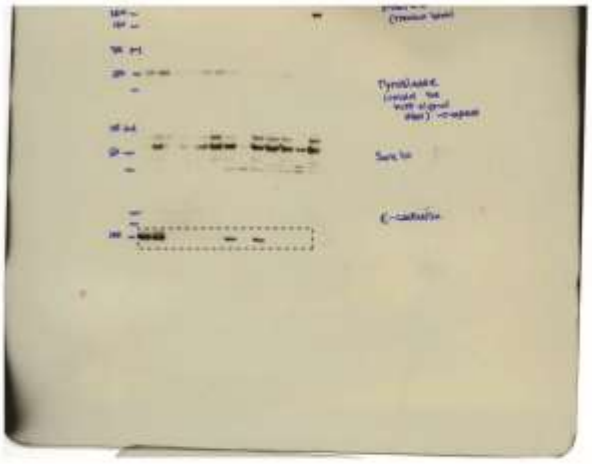

Figure 4C (beta-tubulin in 888Mel (P/R), A375(P/R), D10(P/R), SkMel28(P/R), Colo679(P/R), WM266-4 (P/R) (left to right))

Figure 4C (N-Cadherin in 888Mel (P/R), A375(P/R), D10(P/R), SkMel28(P/R), Colo679(P/R), WM266-4 (P/R) (left to right))

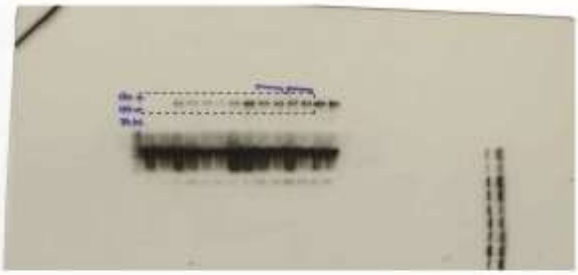

Figure 4C (Fra-1 in 888Mel (P/R), A375(P/R), D10(P/R), SkMel28(P/R), Colo679(P/R), WM266-4 (P/R) (left to right))

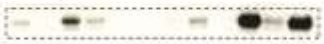

Figure 4F (Fra-1, HSP90 (to bottom) in SkMel28R

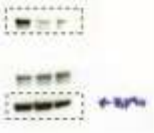

Figure 4F (Fra-1, HSP90 (to bottom) in WM244-4R

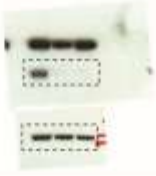

Figure 5A (MITF, SOX10, MelanA (to bottom) in D10, 888mel, 00.08, 06.04, 93.15.2, 94.03, 96.03, SkMel28, 93.03, 607B, A375, A875, 04.04, 04.07, 06.33, 95.23, 518.A2 (left to right))

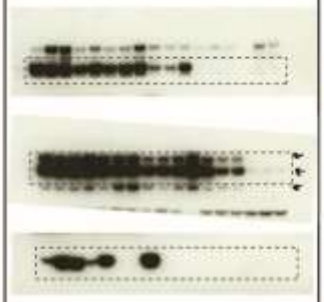

Figure 5A (CDK2, HSP90, SOX10 (to bottom) in D10, 888mel, 00.08, 06.04, 93.15.2, 94.03, 96.03, SkMel28, 93.03, 607B, A375, A875, 04.04, 04.07, 06.33, 95.23, 518.A2 (left to right))

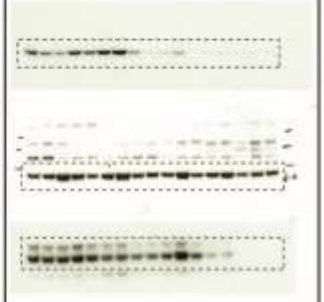

Figure 5C (PARP in D10, SkMel28, A875, D10(+,-), 06.06 (+,-), 96.03 (+,-), left to right)

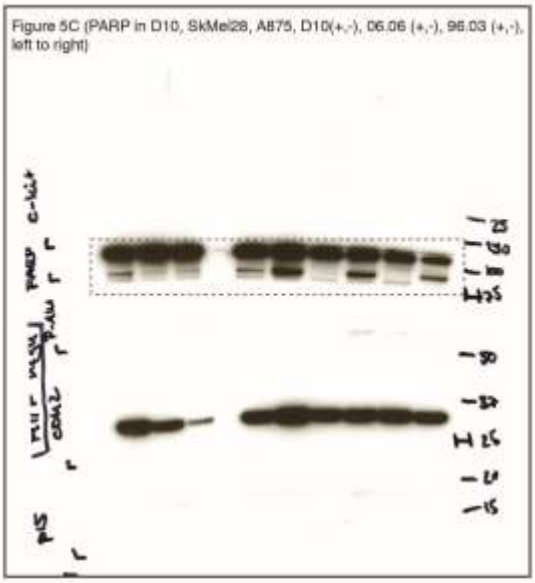

Figure 5C (PARP in D10, SkMel28, A875, A875(+,-), 06.33 (+,-), 04.04 (+,-), left to right)

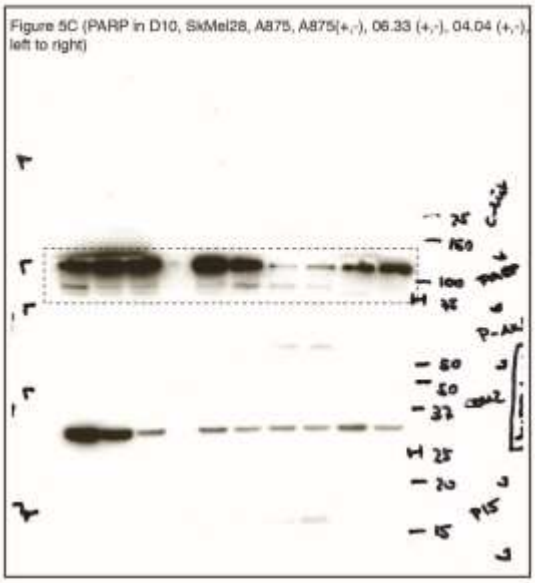

Figure 5C (HSP90 in D10, SkMel28, A875, A875(+,-), 06.33 (+,-), 04.04 (+,-), left to right)

Figure 5C (HSP90 in D10, SkMel28, A875, D10(+,-), 06.06 (+,-), 96.03 (+,-), left to right)

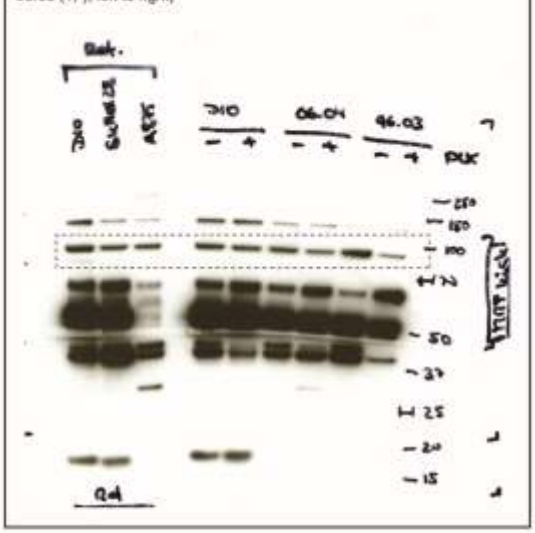

Figure 5C (MITF, P-ERK (from top to bottom) in D10, SkMel28, A875, D10(+,-), 06.06 (+,-), 96.03 (+,-), left to right)

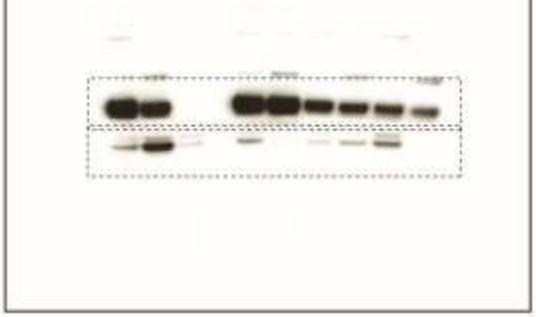

Figure 5C (MITF, P-ERK (from top to to bottom) in D10, SkMel28, A875, A875(+,-), 06.33 (+,-), 04.04 (+,-), left to right)

Figure 6B Phospo-RTK array of Mel888 (top), Mel888+PLX (2nd from top), 518.A2 (3rd from top), 518.A2+PLX (bottom)

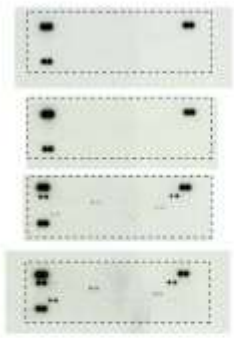

Figure 6C (AXL, HSP90, MITF (from top to bottom) for D10, 888mel, 00.08, 06.04, 93.15.2, A375, SkMel28, 93.03, 607B, A875, 04.04, 04.07, 06.33, 95.23, 518.A2 (left to right)

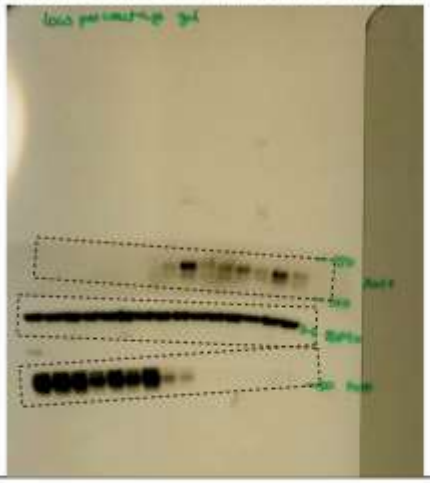

Figure 7D Phospho-RTK array od SkMel28 (top) and SkMel28R (bottom

Figure 6C (EGFR, PDGFRbeta (from top to bottom) for D10, 888mel, 00.08, 06.04, 93.15.2, A375, SkMel28, 93.03, 607B, A875, 04.04, 04.07, 06.33, 95.23, 518.A2 (left to right)

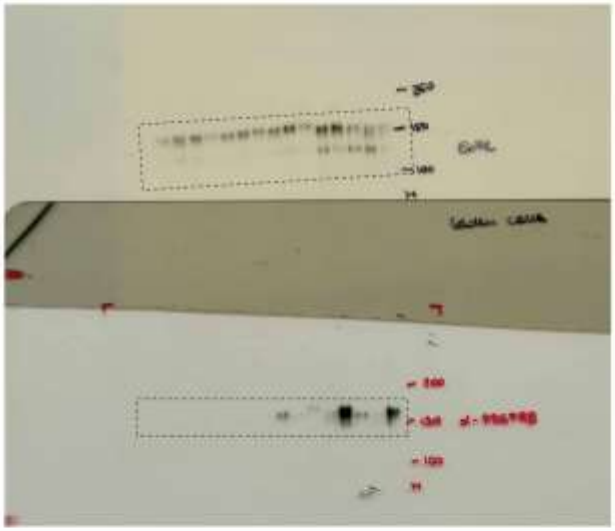

Figure 6C Phospho RTK array of 99.08 (top) and 02.02 (bottom)

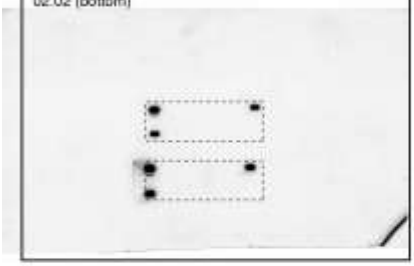

Figure 6D AXL, HSP90, MITF, CDK2, MelanA (from top to bottom) in PDX

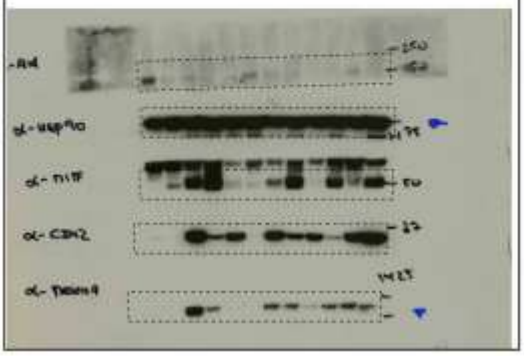

Figure 6D PDGFRbeta, SOX10 (from top to bottom) in PDX

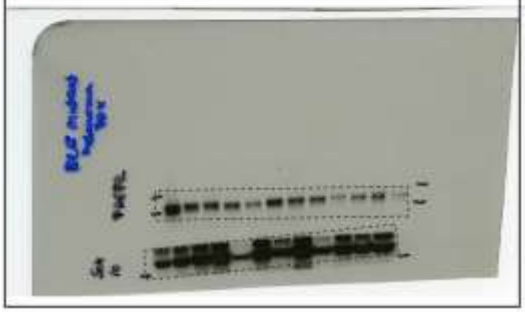

Figure 7C AXL in 888Mel (P/R), A375(P/R), D10(P/R), SkMel28(P/R), Colo679(P/R), WM266-4 (P/R) (left to right))

Figure 7C CDK4 in 888Mel (P/R), A375(P/R), D10(P/R), SkMel28(P/R), Colo679(P/R), WM266-4 (P/R) (left to right))

Figure 7C EGFR, MITF (to bottom) in 888Mel (P/R), A375(P/R), D10(P/R), SkMel28(P/R), Colo679(P/R), WM266-4 (P/R) (left to right))

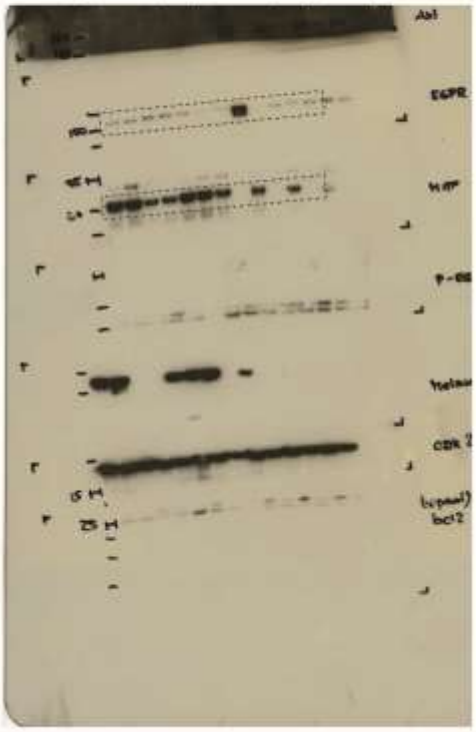

Figure 7C PDGFRbeta in 888Mel (P/R), A375(P/R), D10(P/R), SkMel28(P/R), Colo679(P/R), WM266-4 (P/R) (left to right))

Figure 8B PDGFRbeta, HSP90, SOX10, CDK2, AXL, MITF (from top to bottom) inSkMel2, 99.08, MZ2-Mel, FM6, 01.12, 02.02, 90.07, WM1366A, WM1366B, M016.x1, SkMel147, BLM (left to right)

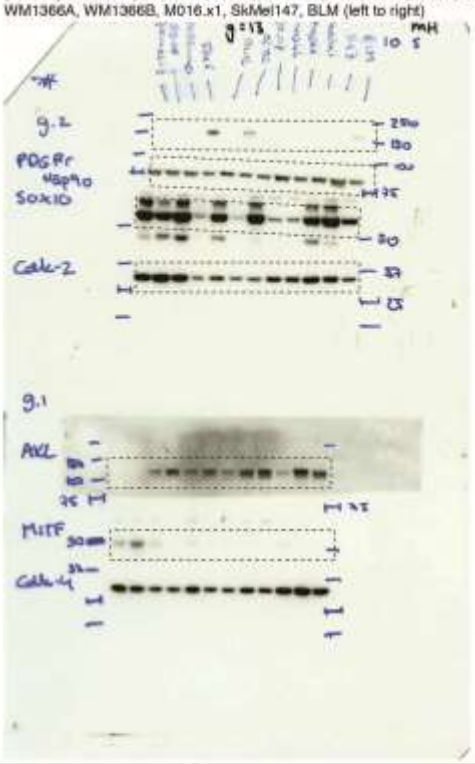

Figure 8H PDGFRbeta, , HSP90, MITF, CDK2, MelanA (from top to bottom, first row), EGFR, SOX10 (to bottom, second row) in SkMel2 and SkMel2R

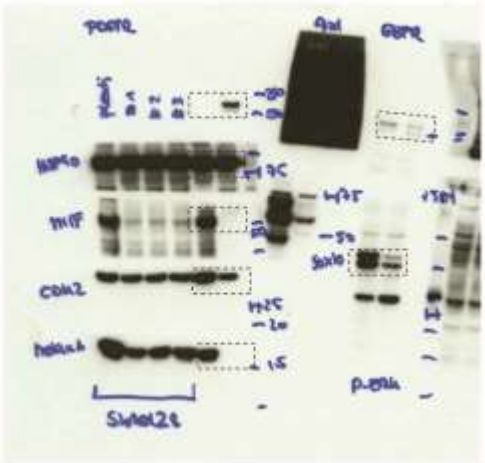

Figure 8H AXL in SkMel2 and SkMel2R

Figure 8B EGFR in SkMel2, 99.08, MZ2-Mel, FM6, 01.12, 02.02, 90.07, WM1366A, WM1366B, M016.x1, SkMel147, BLM (left to right)

Figure 8H P-ERK in SkMel2 and SkMel2R